Features of duplex microstructural evolution and mechanical behavior in the titanium alloy processed by equal-channel angular pressing**

By *Irina P. Semenova, Grigory S. Dyakonov, Georgy I. Raab, Yulia F. Grishina, Yi Huang, Terence G Langdon**

[*]   *I. P. Semenova, G. S. Dyakonov, G. I. Raab, Y. F. Grishina*
Institute of Physics of Advanced Materials, Ufa State Aviation Technical University, 12 K. Marx str., Ufa 450008, Russia
E-mail: Dgr84@mail.ru
        Prof. Terence G Langdon, Y. Huang
Materials Research Group, Faculty of Engineering and the Environment, University of Southampton, Southampton SO17 1BJ, UK

Abstract

This report describes a study of the regularities in the kinetics of microstructure evolution and recrystallization processes in the Ti-5.7Al-3.8Mo-1.2Zr-1.3Sn alloy (Russian analogue VT8M-1) during processing by equal-channel angular pressing (ECAP). To produce a duplex (globular-lamellar) structure, the billets were subjected to preliminary heat treatment, including water-quenching from a temperature below the β-transus followed by annealing at 700°C. For the ECAP temperature selection, the deformation behavior of the alloy with a duplex structure was investigated under upsetting in the temperature range of 650-800°C. The evolution of the globular and lamellar fractions was examined during ECAP processing, and an emphasis was placed on the role of phase transformations, dynamic recrystallization and spheroidization of the α-phase which is realized with increasing accumulated strain when processing by ECAP. It is demonstrated that after 6 ECAP passes an equiaxed ultrafine-grained structure is formed with a mean α-phase grain/subgrain size of ~0.6 μm. The investigation includes an examination of the effect of microstructure on the mechanical properties of the alloy.

Keywords: Duplex structure; Grain refinement; Mechanical properties; Recrystallization; Ti alloy.

1. Introduction.

Two-phase titanium alloys are widely applied in mechanical engineering, especially in the aerospace industry, due to their high specific strength and corrosion resistance. Among commercial two-phase titanium alloys, the most popular is the Ti-6Al-4V alloy owing to its successful alloying.[1, 2] Aluminum in Ti alloys enhances the strength and heat-resistant properties and vanadium stabilizes the β-phase and enhaces the ability of the α-phase to plastic deformation at the expense of the c/a ratio reduction in the HCP lattice. [3] In addition, the low-alloyed Ti-6Al-4V has a lower heat resistance compared to other two-phase and near α-titanium alloys aith a maximum operating temperature not higher than 350°C.[4] It is well known that good high-temperature strength and creep resistance properties are usually obtained during alloying of Al and neutral reinforcers Zr, Sn, Si.[5,6] In particular, the two-phase alloy Ti-5.7Al-3.8Mo-1.2Zr-1.3Sn (Russian analogue VT8M-1), while having the same level of strength as the Ti-6Al-4V alloy, has a lower sensitivity to stress concentrations and an enhanced thermal stability at operating temperatures.[4] Therefore, it can be applied for the production of items operating under high loads and at temperatures up to 450°C. Recently, this alloy has attracted much attention from the designers and manufacturers of parts of gas turbine engines because it successfully substitutes the less heat-resistant and thermally stable alloy Ti-6Al-4V.

By contrast, in modern engineering developments an enhancement of performance properties of structural titanium alloys remains a topical task. It is known that a wide range of properties can be achieved in Ti alloys through a control of the processing history and microstructure. Recent studies demonstrated that the formation of ultrafine-grained (UFG) structures by severe plastic deformation (SPD) processing is an effective way for improving the physical and mechanical properties of commercial metals and alloys.[7, 8] In practice, SPD processing introduces very high plastic strains at relatively low temperatures (usually ~0.3 to 0.4 of the absolute melting temperature) under conditions of high applied pressures.[8] Generally, SPD-produced UFG metals and alloys have grain sizes in the range of ~100-500 nm but they contain different nanostructural

elements in the interiors of the grains including nanotwins, nanoparticles and segregation. This produces a significant effect on their properties and therefore such material features are related to bulk nanostructured materials.[9] For example, the formation of a bulk UFG structure in the Ti-6Al-4V alloy by SPD processing permits an increase in their strength-to-weight ratio, fatigue resistance and fatigue life so that it becomes possible to enhance the service properties of items produced from this alloy.[10-16] Thus, it is reasonable to anticipate that an increase in strength and fatigue resistance due to UFG structure formation in the VT8M-1 alloy will also permit more efficient applications in the design of aircraft engines.

It is well known that titanium alloys generally have a rather low plasticity and therefore in most cases the deformation processing by SPD is conducted at elevated temperatures.[10] For example, processing by equal-channel angular pressing (ECAP) of the Ti-6Al-4V alloy is normally conducted in the temperature range of 600-700°C which is related to features of the stress-strained state under deformation by simple shear.[14,15] Through comparisons of the results of microstructure refinement in titanium and the Ti-6Al-4V alloy processed using various SPD techniques, it was demonstrated that the deformation procedure, temperature, force applied during processing, and the nature of the initial structure all have a significant effect on the shape and size of the formed grains, the phase ratio and the boundary states.[17-19]

The VT8M-1 alloy, as with the Ti-6Al-4V alloy, refers to a class of two-phase $\alpha+\beta$ Ti alloys and its molybdenum equivalent $[Mo]_{eqv}$ is higher than for the Ti-6Al-4V alloy (~2.9 and ~4.0 wt.%, respectively) which ensures an almost 2-fold increase in the fraction of the β-phase at room temperature (~15 and ~30 %, respectively). [1, 2] It is known that with the increasing quantity of β-stabilizers after quenching of two-phase alloys it is possible to form α''-martensite with an orthorhombic lattice, the decomposition of which normally leads to the maximum effect of aging in the alloy and often produces a strong decrease in ductility.[1] There is also significant information on the hexagonal close-packed to face-centered cubic phase transformation in the Ti-6Al-4V alloy during SPD processing.[20]

2

There are differences in alloying between the Ti-6Al-4V and VT8M-1 alloys. The VT8M-1 alloy is doped with tin (~1.3Sn) and zirconium (~1.2Zr) whereas there is no tin in the Ti-6Al-4V alloy and the Zr content is very low (less than 0.3 % wt.%). Doping of Ti alloys with Zr and Sn favorably affects the heat resistance but also it decreases the ductility of the alloy. Thus, the composition of doping elements of the VT8M-1 alloy and the features of phase transformations in the VT8M-1 alloy may have a significant effect on the deformability at elevated temperatures. Therefore, although the Ti-6Al-4V and VT8M-1 alloys are similar, the deformation regimes of the Ti-6Al-4V alloy are not suitable for VT8M-1.

The present research was focused on determining the deformation conditions, in terms of temperature and strain, for producing defect-free billets by ECAP and studying the characteristic features of the UFG structure formation in the VT8M-1 alloy. For this purpose, the alloy deformability was studied on small-sized samples under upsetting in the temperature range of 650 to 800°C. Thereafter, the bulk billets of the alloy were subjected to multi-pass ECAP in order to produce a UFG structure, and the mechanisms of structural and phase transformations were studied by X-ray diffraction analysis and transmission electron microscopy (TEM).

2. Experimental material and procedures

A rod of the VT8M-1 alloy (Ti-5.7Al-3.8Mo-1.2Zr-1.3Sn in wt.%) manufactured by VSMPO-AVISMA (Russia) was selected as the material for this study. The rod had a diameter of 25 mm and the temperature of the β-transus was 980°C. The initial billets were heated at 940°C, water-quenched and then annealed at a temperature of 700°C for 1 h and air-cooled to produce a duplex (globular-lamellar) structure. In order to evaluate the alloy deformability, cylindrical samples with diameters of 6 mm and heights of 8.5 mm were subjected to compression testing under isothermal conditions in the temperature range of 650-800°C at a strain rate of 1.4×10^{-3} s^{-1} in air using an Instron testing machine operating under a constant rate of crosshead displacement up to engineering strains of $\varepsilon = 50$ %. All microstructure examinations were conducted in the

billet centre.

After heat treatment, the billets were subjected to 2, 4 and 6 ECAP passes using an angle within the ECAP die of φ = 120° with a temperature of 750°C via route B_C, in which the billet is rotated by 90° in a clockwise sense between consecutive passes. The ECAP facility used in this work was equipped with a die heated to a temperature of 550°C in order to provide the isothermal conditions for billet straining. The total time spent for the billet placement in the ECAP die-set and ECAP processing was no more than 1.5 minutes. Taking into account the comparatively fast ECAP deformation (4 mm/s) and deformation heating, it is anticipated that the billet temperature may drop below 700°C where this lower temperature may lead to reduced deformability on the next pass through the die. Therefore, prior to a subsequent pass the billet was heated at 750°C for 30 minutes to ensure a uniform temperature.

The strain produced in each pass, ε_n, was calculated according to the relationship[21]

$$\varepsilon_n = \frac{2}{\sqrt{3}} ctg\left(\frac{\varphi}{2}\right) \tag{1}$$

Cylindrical specimens with diameters of 3 mm and gauge lengths of 15 mm were used for the tensile testing. These tensile tests were conducted at a strain rate of 1.0×10^{-3} s^{-1} at room temperature on an Instron testing machine.

The sample microstructures after ECAP were studied in the cross-sections of the billets. Since the shear direction is changed after each ECAP pass, then on the SEM images of microstructures the arrows indicate the shear direction only for the most recent pass of ECAP.

The microstructures in the longitudinal sections of various samples were analyzed by scanning electron microscopy (SEM) using a JEOL JSM 6390 microscope and by TEM. Foils for the TEM examinations were prepared by electrical discharge machining, mechanically thinned to a thickness of ~100 μm and then electro-polished using a TenuPol-5 facility a solution of 5% perchloric acid, 35% butanol and 60% methanol, at a polishing temperature in the range from –20 to –35°C. The microstructures were examined using a JEOL JEM 2100 microscope operating

with an accelerating voltage of 200 kV.

The X-ray diffraction (XRD) analysis was conducted on a Rigaku Ultima IV diffractometer. The samples were examined with CuK_α-radiation (40 kV, 30 mA) and the phase composition of the alloy was determined using the Rietveld method. In this procedure, an iterative refinement of the initial estimates of the profile and structural parameters is prepared during adjustment of the theoretical profile of the diffraction pattern in order to match the experimental data.[22] The accuracy of the measurements in this procedure was estimated as ±2 %.

3. Experimental results

3.1 Microstructure of the VT8M-1 alloy after preliminary heat treatment

Figure 1 displays a representative microstructure of the alloy in the as-received state. The microstructure consists of grains of the primary α-phase with a size of about 5 μm and having a volume fraction about 65%. The remainder of the billet volume consists of a plate-like α+β structure. It was shown earlier that the most effective grain refinement in the two-phase Ti-6Al-4V alloy during ECAP occurs in the plate-like morphology structure. The retention of the fraction of the primary α-phase at no less than 25% ensures a satisfactory deformability during severe plastic deformation.[23] This approach was used for the two-phase VT8M-1 in the current work.

Figure 2a shows a typical SEM image of the alloy structure after quenching. Inspection shows that within the microstructure there is a martensitic structure and grains of the primary α_p-phase with the fraction of the latter of the order of about 25%. The morphology of the martensitic structure in the TEM image in Figure 2b indicates the formation of α'' martensite plates containing, as shown in Figure 1c, many twins, dislocations and stacking faults.

After heating of the quenched alloy at 700°C for 1 h, the microstructure consisted of α_p-phase grains with globular morphology and $\alpha+\beta$ regions having a lamellar structure. This is clearly seen in the SEM image of the microstructure presented in Figure 3a. The fraction of the globular α-phase was estimated as about 25%, the average globular size was ~2.7 μm and the average thickness of the α-plates was ~0.12 μm as shown in the TEM image in Figure 3b.

5

According to the data from *X*-ray phase analysis, the fraction of the β-phase at room temperature was ~12%, and this is much smaller than the fraction of ~30% in the equilibrium as-annealed state.[4] Evidently, the lower fraction of ~12% after quenching and heating may be associated with an incomplete decomposition of martensite. It is known that the decomposition of *α″* martensite in alloys of the Ti-4% Mo system occurs via a spinodal decomposition mechanism, where before the final precipitation of the β-phase there forms a non-equilibrium modulated structure consisting of depleted $α″_{lean}$ and enriched $α″_{rich}$ martensite.[1] It appears, therefore, that heating for 1 h was insufficient to produce a complete decomposition of the martensitic structure. In addition, it was impossible to identify their quantitative ratio by means of XRD.

3.2 The deformability of the VT8M-1 alloy and selection of an ECAP processing regime

The engineering curves presented in Figure 3 show the change in the stress during compression of the samples at temperatures from 650 to 800°C. An increase in temperature from 650 to 800°C leads to a reduction of the stress at the stage of steady flow from ~580 to ~155 MPa and an increase in its duration. No hardening at upsetting is connected with development of dynamic processes of recovery and recrystallization which maintain a constant level of the dislocation density during deformation.[24] A reorientation of α-phase plates at the initial stage of compression can contribute to some softening of the alloy.[25]

It was noted also that the most active rotation of α-plates in the Ti-6Al-4V alloy occurred at strains of about 0.3.[26] Such mechanical behavior is typical of *a+β* titanium alloys with a lamellar structure, in particular for the Ti-6Al-4V alloy.[25-28] It follows from the microstructure studies as in Fig. 4 that the growth of the compression temperature leads to an increase in the thickness of α-phase plates and the sizes of the globular particles. This demonstrates the development of spheroidization of the alloy exactly during plastic deformation. As with the Ti-6Al-4V alloy, the deformation temperature growth applied to VT8M-1 does not lead to an increase in the fraction of the globularized microstructure.[25]

The smallest values of flow stress were observed at 750 and 800°C, but during heating at

6

800°C the process of structure recrystallization will not give efficient grain refinement during ECAP. Therefore, from the compression tests of the samples, a deformation temperature of 750°C was chosen for further investigation and for the ECAP processing of bulk billets where it is assumed there is heating of a billet prior to deformation and between ECAP passes. In the present investigation, during the whole ECAP process (from 1 to 6 passes) the total duration of billet heating can achieve 3 hours. It is known that globularization of the microstructure of two-phase Ti alloys can develop during static heating within certain temperature ranges.[3] In order to exclude the impact of static heating at 750°C on a possible spheroidization of the α-plates, a check experiment was carried out. Figure 5 displays the microstructure of the VT8M-1 alloy after heat treatment (Fig. 5a) and additional heating of the billet at T=750°C for 4 hours (Fig. 5b). It is noted that after annealing the cross sizes of the plates increase but no transformation of lamellar microstructures to a globular morphology occurs in the alloy.

It is reasonable to expect that the heating of the billets at a temperature of 750°C before processing and between the ECAP cycles will lead to a completion of decomposition of the α″ martensite formed after the preliminary heat treatment.

3.3 Microstructure evolution in the VT8M-1 alloy during ECAP processing

The microstructe studies were performed after 2, 4 and 6 ECAP passes which produced equivalent strains in the billet equal to 1.4, 2.8 and 4.0, respectively.

Figure 6a shows the SEM image of the microstructure after 2 ECAP passes. It can be seen that there is a division of the α-phase plates followed by the formation of particles close to an equiaxed shape. The character of the formed microstructure indicates the development of lamellar spheroidization, accompanied initially by the fragmentation of plates by shear bands or via the formation of dislocation boundaries.[25]

It is apparent also that the evolution of the spheroidization process is non-uniform. In the microstructure there are coarse non-fragmented plates in addition to nearly equiaxed particles having a size of ~0.1 - 0.7 μm (Figure 6 b,c). The average size of the spheroidization particles

7

was estimated as ~0.34 μm. It is known that plates oriented perpendicularly to the flow direction undergo the most intensive changes.[28] The primary globular α-phase grains have become somewhat elongated in the direction of deformation but their average size has not changed compared to their initial state and it was measured as ~2.7 μm. It can be seen in the TEM images in Figures 6 b and c that separate fragmented plates contain both an increased dislocation density and some low-angle boundaries as in Figure 6c whereas within the primary α-phase there is a grain-subgrain mixture in Figure 6b.

The XRD data in Table 1 demonstrate that even after 2 ECAP passes the dislocation density increases from ~0.6 to ~1.4 × 10^{15} m^{-2} and the size of the coherent-scattering regions (CSR) decreases almost two-fold from ~90 to ~55 nm. At the same time, there is an increase in the fraction of the β-phase from ~12 to ~40%. This is attributed to the completion of the $α''$-martensite decomposition and the formation of an equilibrium α+β structure resulting from the heating of the billets to 750°C prior to ECAP and SPD which promotes martensitic decomposition.

After 4 ECAP passes the lamellar fraction almost fully transforms into an equiaxed configuration as is apparent in Figure 7a. The size of spheroidizied particles varies within the range of ~0.1 to ~1.0 μm (according to SEM - fig 7a) and the average size of grains/subgrains is ~0.48 μm (according to TEM fig 7b). The average size of the weakly deformed primary $α_p$-phase remains unchanged at –2.7 μm. The TEM image in Figure 7 b shows some fragments of the plates remain. Within the $α_p$-phase grains there are new low-angle grain boundaries (LAGBs) but the local misorientations of the subgrain boundaries increase and separate fragments with a size of ~1 μm and larger are observed as in Figure 7c.

After 6 ECAP passes the strain increases to ~4.0 and the $α_p$-grains assume an elongated shape but their average sizes remain practically unchanged at ~2.6 μm. However, the average size of the equiaxed α-particles increases from ~0.48 to ~0.70 μm in Figure 8 a,b. A similar tendency was observed when the CSR sizes were evaluated by XRD where after 6 ECAP passes their size

increased to ~60 nm compared to ~48 nm after 4 passes. Furthermore, the dislocation density increased with straining and after 6 ECAP passes the density was ~1.9×10^{15} m^{-2} (Table 1). A slight increase in the dislocation density in the material, which is observed with increasing numbers of passes, is evident the expense of dislocations increments in the primary globular α-phase and this accumulates the strain and is not subjected to recrystallization during ECAP. An increase of α-particles sizes after ECAP may occur due to the active development of dynamic recrystallization and spheroidization at these elevated temperatures. However, the volume fraction of the β-phase consistently decreased from ~40 to ~22% with increasing strain where this is attributed to the dissolution of the metastable β-phase as induced by SPD. Similar regularities in the transformation of the metastable β-phase were also observed in the Ti-6Al-4V alloy with increasing strain during HPT processing.[17]

3.4 Mechanical properties of the VT8M-1 alloy after ECAP processing

Table 2 shows the variation of the ultimate tensile strength with the number of ECAP passes. An enhancement in strength is observed after 2 passes from ~1050 to ~1200 MPa where this is due to the increase in the dislocation density, the formation of new strain-induced grains and the decrease in the value of CSR by almost 2 times (from 90 to 54 nm). It is known that α″-martensite is a more "soft" phase compared to α and α '-martensite [3] . Therefore, it appears that the decay of α″-martensite during 2 passes of the ECAP leads to the formation of a mixture of ultra-fine grains of α+β-phases which can contribute to additional hardening of the material.

A further increase in strain from 4 to 6 passes leads to a reduction in the UTS which is associated with features of the microstructural transformation due to the development of recrystallization, spheroidization processes and an increase in the average size of the α-particles in (α+β) regions as shown in Figures 7 and 8. The apparent slight softening with an increase in the number of passes to 6 is due to the fact that the volume fraction of the recrystallized α + β region is significantly larger than for the non-recrystallized primary α- phase with an increased dislocation density.

9

Figure 9 shows typical tensile curves at room temperature for the samples from the heat-treated alloy having a duplex microstructure and for those after 6 ECAP passes having a UFG structure with α-phase grains having an average size of ~0.6 μm. Thus, the UFG structure in the alloy leads to an increasing UTS while the elongation is reduced only slightly from ~15% and ~11% in the coarse-grained alloy and the UFG alloy, respectively.

4. Discussion

These experiments demonstrate the possibility of producing a UFG structure in the VT8M-1 alloy through ECAP processing. When selecting the processing regime, the approach consisted of a preliminary preparation of the structure by heat treatment where this resulted in the formation of a duplex or bimodal structure raising the efficiency of grain refinement during ECAP processing. Thus, in the $(\alpha+\beta)$ region with a lamellar structure there was formed a homogeneous UFG structure occupying about 75% of the volume whereas in the primary α-phase grains the dislocation motion led to the formation of weakly-misoriented substructures which in aggregate ensured a combination of high strength and reasonable ductility.[16] In the present research, a duplex structure was produced in the VT8M-1 alloy by quenching from a temperature below the β-transus with subsequent high heating at 700°C for 1 hour.

At the same time, some features of the phase transformations were revealed in the VT8M-1 alloy during heat treatments which were different from those in the Ti-6Al-4V alloy. For example, there was the formation of an orthorhombic α'' martensite after water-quenching. It is known that the decomposition of the α'' martensite during subsequent aging provides the maximum strengthening effect.[1] In this connection, and in order to preserve the plasticity of the billet, a high temperature of heating of 700°C was selected. As demostrated by these studies, the duration of the heat treatment of 1 hour was not sufficient for a full completion of the martensitic decomposition and in the alloy structure there was a ratio between the α and β phases which was different from the equilibrium ratio.[3] However, and as expected, during the subsequent heating of the billets to a

10

deformation temperature of 750°C and after 2 ECAP passes, the structure was close to an equilibrium phase composition with 40% β and 60% α (Figure 4).

Considering the deformation behavior of the alloy under upsetting, a decrease in flow stress in the VT8M-1 alloy was observed only at temperatures of 750 and 800°C. It should be noted that the dispersal of the initial plates impacts significantly on the development of the α-phase globularization during plastic deformation. The thickness reduction of the α-plates at the expense of faster cooling of the two-phase Ti alloy can considerably reduce the strain degree which is required for complete globularizaion.[25,27,29] In practice, with a 40% upsetting of the Ti-6Al-4V alloy with a thickness of α-phase plates of about 1 μm and subsequent annealing at sufficiently high temperatures (815°C), it was shown that such plates of the α-phase did not globularize during annealing.[25] In the present work, a more thin plate structure with a thickness of α-plates of ~0.2 μm was formed in the VT8M-1 after heat treatment, and it is evident that this made the fragmentation and globulariation easier in the conditions of warm upsetting.

In addition, the globularization of the α-phase plates at upsetting of the VT8M-1 alloy developed non-uniformly across the sample section, and this is apparently connected with their different orientations against the material flow direction.[25] Thus, the results obtained for the VT8M-1 sample upsetting showed that the most appropriate temperature for ECAP was 750°C. Accordingly, and in order to retain the material deformability during repeated ECAP passes, the billets were subjected to heating between the passes at the same temperature for 30 minutes.

It should be noted that in the present work the ECAP processing of the alloy was conducted at a relatively high temperature of 750°C as opposed to the well-studied Ti-6Al-4V alloy. An earlier report showed that Ti-6Al-4V samples with a diameter of 20 mm were processed in the die-set via the developed regimes with preliminary heat treatment and ECAP processing (2 and 6 passes) at 650°C.[23] Figure 10 displays the microstructures of the Ti-6Al-4V billets after ECAP at T=650°C with accumulated strains of at least ~4.

Studies of microstructure transformation with increasing strain in the VT8M-1 alloy

11

during ECAP processing revealed several similar effects to those observed earlier in the Ti-6Al-4V alloy: specifically, a destruction and spheroidization of the α-phase plates which leads to the formation of equiaxed ultrafine grains/subgrains and a fragmentation of the primary α-phase grains with the formation of a wealky-misoriented substructure.[30, 31] It is also interesting to note the difference in the evolution of the phase compositions of the Ti-6Al-4V and VT8M-1 alloys. Figure 11 demonstrates that after preliminary heat treatment the fraction of the β-phase is almost the same in both alloys and is about 12%. Further deformation of Ti-6Al-4V by ECAP leads to the decrease in the fraction of the β-phase to 7.6 % after 2 passes and this contrasts with the VT8M-1 alloy in which the fraction of the β-phase after the first passes increases by up to 40%. This is explained because the Ti-6Al-4V alloy in the heat-treated state was in the equilibrium state whereas the VT8M-1 alloy was in a non-equilibrium state as it contained the undecomposed α''-martensite.

It is important to note also that in the VT8M-1 alloy ultrafine equiaxed grains of the α-phase form already when the accumulated strain reached ~2.8, corresponding to 4 ECAP passes (Fig 7), whereas in the Ti-6Al-4V alloy at a temperature of 650°C the minimum strain required for the formation of a homogeneous UFG structure was at least ~4 (Fig. 10b).[30, 32] Apparently, in the VT8M-1 alloy the formation of α'' martensite plates, having within them a large number of twin boundaries and stacking faults, facilitated the processes of spheroidization of plates and the formation of new boundaries during subsequent deformation by ECAP.

Considering the mechanical behavior of the VT8M-1 alloy with increasing numbers of passes, it is noted that the UTS of the alloy increases after 2 passes compared to the initial heat-treated state (from 1030 to 1200 MPa) and this is due both to a refinement of the α-plates and an increase in the dislocation density. However, a subsequent increase in accumulated strain during ECAP processing from ~1.4 to ~4.0 leads to a consistent decline in the UTS to ~1135 MPa. Another situation was observed for Ti-6Al-4V as in Fig. 12. The maximum strength enhancement occurs in the first two ECAP passes and the subsequent increasing strain leads to insignificant

12

hardening and saturation. Such behavior is typical of pure Ti and other materials subjected to ECAP.[21] The non-typical softening of the VT8M-1 alloy with increasing strain is connected with the recrystallization processes which occur during heating of the billet before each ECAP pass at a relatively high temperature (750°C). This is confirmed by the increase in the CSR after 6 ECAP passes as shown in Table 1. A slight increase of the dislocation density with each ECAP pass is conditioned by the fact that the accumulation of dislocations occurs mainly in non-recrystallized grains of the primary α-phase and the X-ray technique evaluates only the integral value of the dislocation density within the material. Finally, the strength characteristics of the UFG alloy remain higher than those in the initial heat-treated state (~1135 and ~1030 MPa, respectivley) and the overall ductility is retained at a level of ~10%.

It is expected that the formation of an equiaxed UFG structure in the VT8M-1 alloy will provide reasonably high deformability at lower temperatures, and thus it will make an additional contribution to the strengthening during subsequent processing operations and/or in the production of commercial semi-products and articles. Such an approach was successfully applied when producing pilot articles such as gas turbine engine blades from the Ti-6Al-4V alloy using low temperature isothermal stamping.[34] In practice, the fatigue strength of such products at room temperature was ~30% higher by comparison with the conventional stamping technology.[33] It is assumed, therefore, that a similar approach may be successfully implemented also for the high-temperature VT8M-1 alloy.

5. Summary and conclusions

1. Experiments were undertaken to investigate the formation of UFG structures in the high temperature VT8M-1 alloy through ECAP processing at a temperature of 750°C. The results show the formation in the alloy of a duplex lamellar-globular structure consisting of primary α-phase grains and a mixture of α and α″ martensite plates.

13

2. As the number of ECAP passes increases from 2 to 6, the transformation of the microstructure proceeds by way of fragmentation of the lamellar fraction with a subsequent spheroidization due to the advent of static and dynamic recrystallization, conditioned by deformation at the elevated temperature and heating of the billets between the passes. The primary α-phase grains retain their initial size and deform with the formation of weakly misoriented dislocation cells.

3. The formation in the microstructure of equiaxed ultrafine grains of the α- and β-phases with a volume fraction of about 75% under an accumulated strain of ~2.8, equivalent to 4 ECAP passes, leads to an increase in ultimate tensile strength from ~1030 to ~1160 MPa and an elongation of ~9,4%. This creates conditions for the subsequent processing of the UFG alloy at lower temperatures and for further strengthening.

4. It is suggested that this approach is promising for producing commercial semi-products and articles having UFG structures and enhanced performance properties.

References

[1] C. Leyens, M. Peters, *Titanium and Titanium Alloys: Fundamentals and Applications*. Wiley-VCH, Weinheim, Verlag GmbH, **2003**, p. 513.

[2] C. Veiga, J.P. Davim, A.J.R. Loureiro, *Rev. Adv. Mater. Sci.* **2012***, 32*, 133.

[3] G. Lütjering, J. C. Williams, *Titanium*, Springer Science & Business Media, **2007**, p. 335

[4] V.G. Antashev, N.A. Nochovnaya, T.V. Pavlova, V. I. Ivanov, *High-temperature titanium alloys.* **2007**, 7. (http://viam.ru/public/files/2006/2006-204686.pdf (in Russian))

[5] C. Anders, G. Albrecht, G. Luetjering, *Z. Metallkd.* **1997**, *88*, 197.

[6] P. Potozky, H.J. Maier, H-J. Christ, *Metall. Mater. Trans. A.* **1998**, *29A*, 2995.

[7] R. Z. Valiev, Y. Estrin, Z. Horita, T. G. Langdon, M. J. Zehetbauer, Y. Zhu, *JOM*, **2016**, *68*, 1216.

[8] R.Z. Valiev, *Nature Mater.* **2004**, *3*, 511.

[9] R.Z. Valiev, T.G. Langdon, *Adv. Eng. Mater.* **2010**, *12*, 677.

[10] S.L. Semiatin, D.P. DeLo, *Materials & Design.* **2000***, 21*, 311.

[11] R.S. Mishra, V.V. Stolyarov, C. Echer, R.Z. Valiev, A.K. Mukherjee, *Mater. Sci. Eng. A.* **2001**, *298*, 44.

[12] S.V. Zherebtsov, G.A. Salishchev, R.M. Galeyev, O.R. Valiakhmetov, S.Yu. Mironov, S.L. Semiatin, *Scripta Mater.* **2004**, *51*, 1147.

[13] H.J. Rack, J. Qazi, L. Allard, R. Valiev, *Mater. Sci. Forum.* **2008**, *584–586*, 893.

[14] I.P. Semenova, E.B. Yakushina, V.V. Nurgaleeva, R.Z. Valiev, *Int. J. Mater. Res.* **2009**, *100*, 1691.

[15] L.R. Saitova, H.W. Hoeppel, M. Goeken, I.P. Semenova, R.Z. Valiev, *Int. J. Fatigue.* **2009**, *31*, 322.

[16] I.P. Semenova, A.V. Polyakov, V.V. Polyakova, Y. Huang, R.Z. Valiev, T.G. Langdon, *Adv. Eng. Mater.* **2016**, *18*, 2057.

15

[17] A.V. Sergueeva, V.V. Stolyarov, R.Z. Valiev, A.K. Mukherjee, *Mater. Sci. Eng. A*. **2002**, *323*, 318.

[18] Y.G. Ko, W.S. Jung, D.H. Shin, C.S. Lee, *Scripta Mater.* **2003**, *48*, 197.

[19] S.M. Kim, J. Kim, D.H. Shin, Y.G. Ko, C.S. Lee, S.L, Semiatin, *Scripta Mater.* **2004**, *50*, 927.

[20] H. Shahmir, T.G. Langdon, *Mater. Sci. Eng. A*, **2017**, *704*, 213.

[21] R. Z. Valiev, T. G. Langdon, *Prog. Mater. Sci.* **2006**, *51*, 881.

[22] D.L. Bish, S.A. Howard, *J. Appl. Cryst*. **1988**, *1*, 86.

[23] I. P. Semenova, L. R. Saitova, G. I. Raab, A. I. Korshunov, Y. T. Zhu, T. C. Lowe, R. Z. Valiev, *Mater. Sci. Forum.* **2006**, *757*, 503.

[24] F. Humphreys, M. Hatherly, in *Recrystallization and related annealing phenomena*, (Eds: D. Sleeman), Elsevier, Oxford, **2004**, p. 574

[25] S.L. Semiatin, V. Seetharaman, I. Weiss, *Mater. Sci. Eng. A*. **1999**, *263*, 257.

[26] S. Zherebtsov, M. Murzinova, G. Salishchev, S.L. Semiatin, *Acta Mater*. **2011**, *59*, 4138.

[27] S.L. Semiatin, T.R. Bieler, *Acta Mater.* **2001**, *49*, 3565.

[28] T.R. Bieler, S.L. Semiatin: *Int. J. Plast*. **2002**, *18*, 1165.

[29] S. V. Zherebtsov, S. Mironov, M. A. Murzinova, S. Salishchev, S. L. Semiatin, *Mater. Sci. Forum.* **2008**, *584—586*, 771.

[30] I.P. Semenova, L.R. Saitova, G.I. Raab, R.Z. Valiev, *Mater. Sci. Eng. A*. **2004**, *387-389*, 805.

[31] S. L. Demakov, O. A. Elkina, A. G. Illarionov, M. S. Karabanalov, A. A. Popov, I. P. Semenova, L. R. Saitova, N. V. Shchetnikov, *The Physics of Metals and Metallography*, **2008**, *105*(6), 602.

[32] I.P.Semenova, L.R.Saitova, R.K.Islamgaliev, T.V.Dotsenko, A.R.Kilmametov, S.L.Demakov, R.Z.Valiev, *The Physics and Metallography***. 2005,** *100(1)*, 77.

[33] I.P. Semenova, G.I. Raab, V.V. Polyakova, N.F. Izmailova, S.P. Pavlinich, R.Z.Valiev, *Rev. Adv. Mater. Sci.* **2012**, *31*, 179.

Table 1. Substructure parameters of VT8M-1 alloy depending on numbers of ECAP passes.

Alloy condition	Average values of coherent-scattering regions (CSR), nm	Fraction of β-phase, %	Dislocation density, 10^{15} m^{-2}
Quenching +heating	90.1	11.9(3)	0.62(5)
2 passes of ECAP	54.8	39.6(6)	1.41(9)
4 passes of ECAP	47.3	26.3(4)	1.58(3)
6 passes of ECAP	59.0	22.4(7)	1.89(7)

Table 2 Mechanical properties of the VT8M-1 alloy depending on numbers of ECAP passes.

Alloy condition	UTS, MPa	YS, MPa	Elongation, %
Quenching +heating	1030	940	12.0
2 passes of ECAP	1208	1134	9.0
4 passes of ECAP	1159	1090	9.4
6 passes of ECAP	1134	1071	10.0

Figures captions.
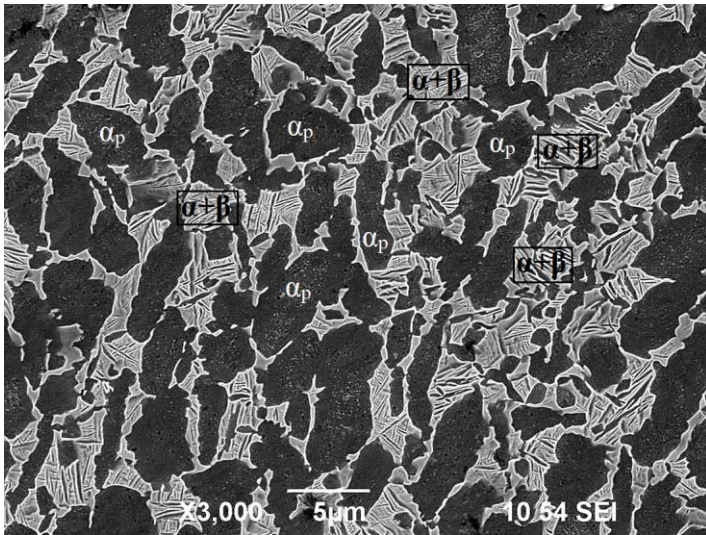
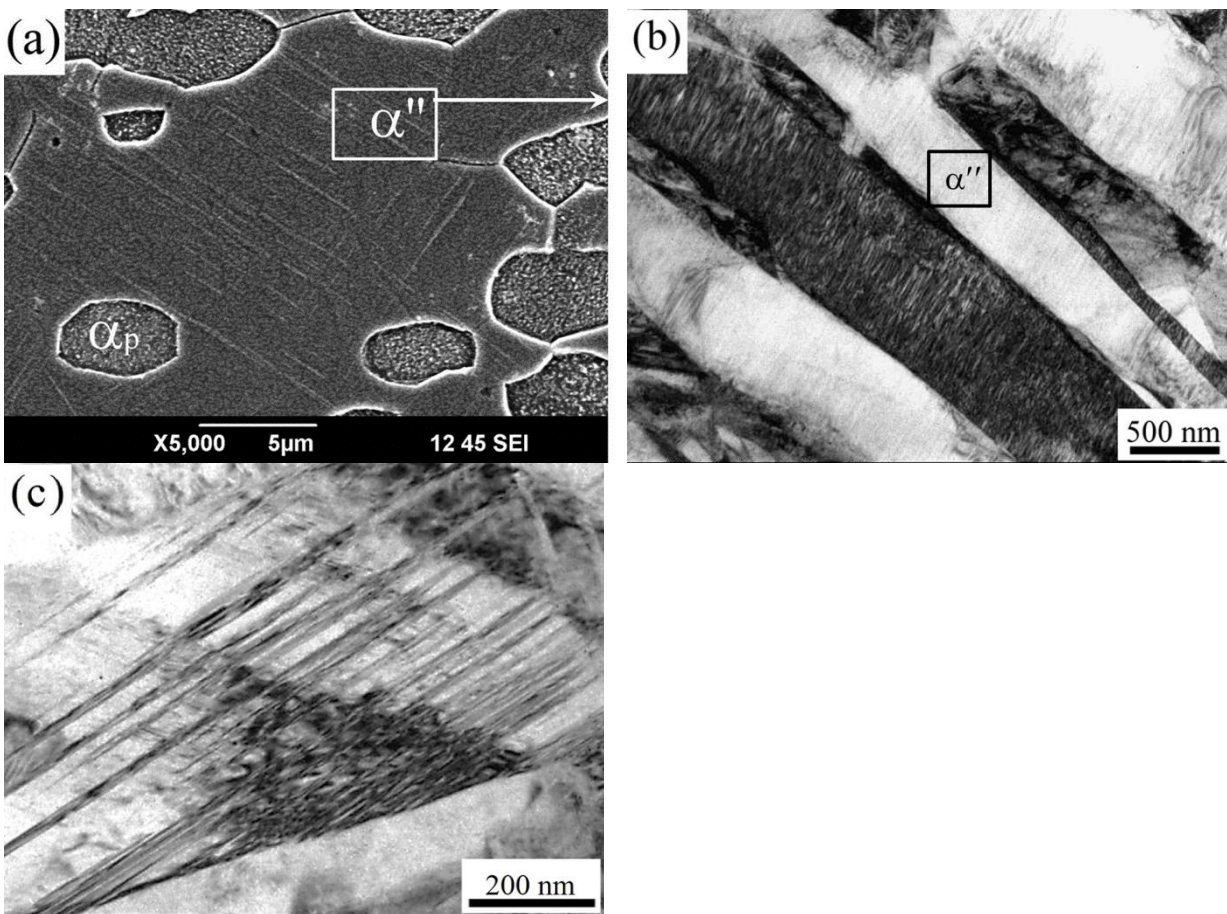Fig. 1. Microstructure of VT8M-1 alloy in the as-received state.

Fig. 2. Microstructure of the VT8M-1 alloy after quenching at 940°C showing α_p and α'' regions: (a) - SEM and (b,c) - TEM.
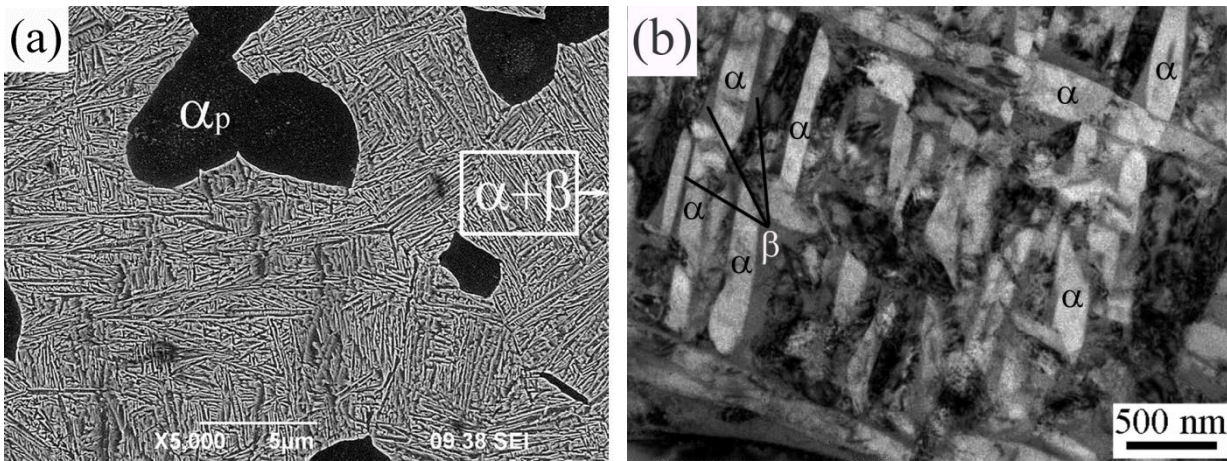
Fig. 3. Globular-lamellar structure of the VT8M-1 alloy after heat treatment at 700°C for 1 hour using (a) - SEM and (b) - TEM.
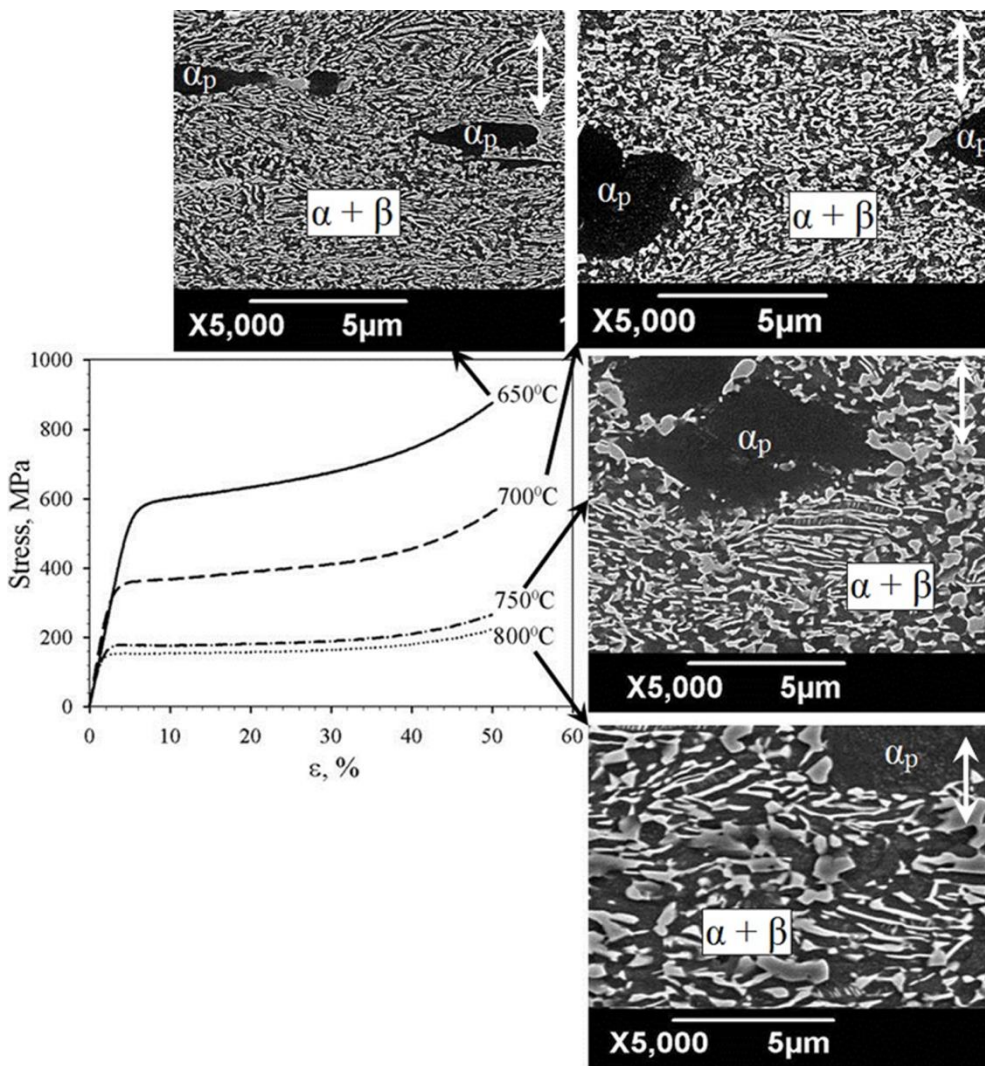
Fig. 4. Engineering stress versus strain during compression of the VT8M-1 alloy at temperatures from 650 to 800°C using a strain rate of $1.4 \times 10^{-3}\,\text{s}^{-1}$ and corresponding microstructure.
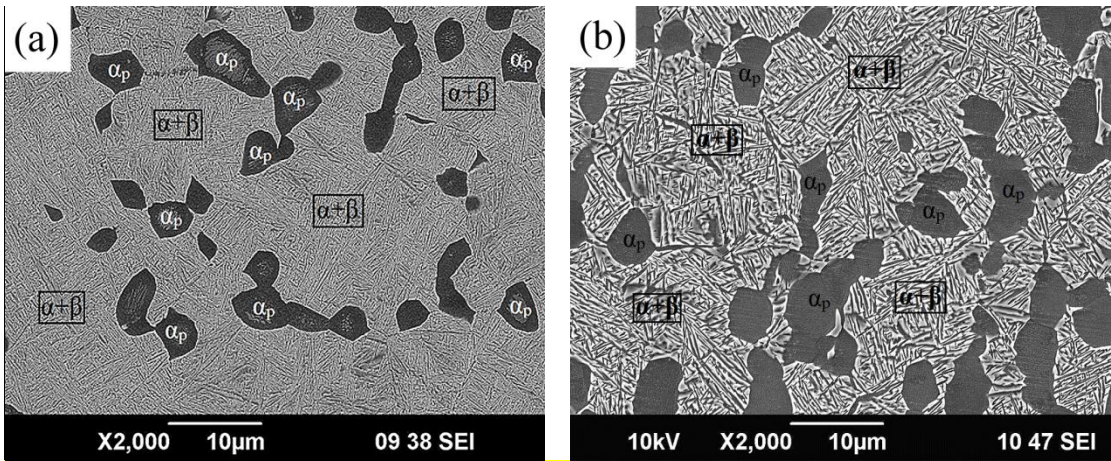
Fig. 5. (a) Microstructure of VT8M-1 alloy after preliminary heat treatment (heated at 940°C, water-quenched and annealed at 700°C for 1 h) and (b) additional annealing at T=750°C for 4 h
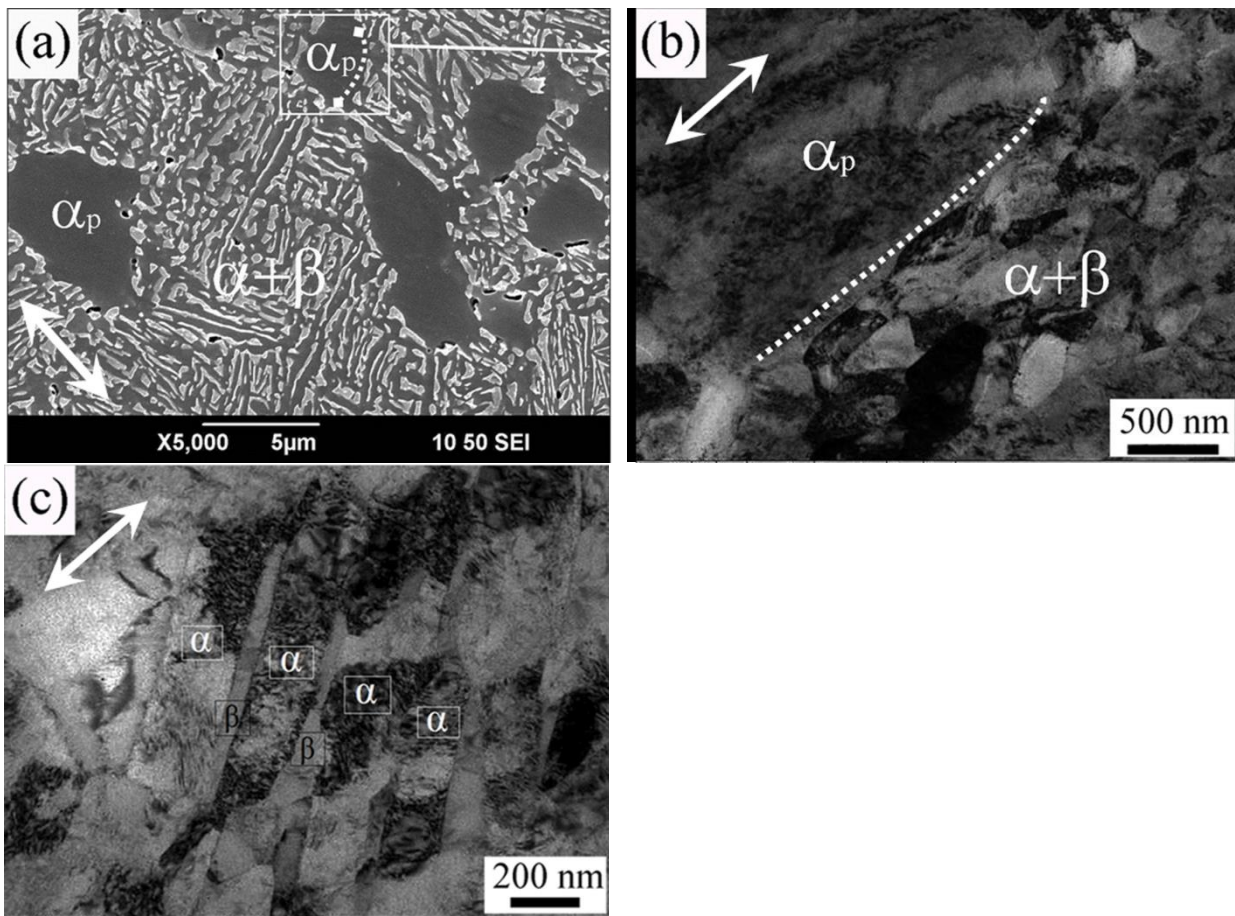
Fig. 6. Microstructure of the VT8M-1 alloy after ECAP processing for 2 passes showing the α_p phase and $\alpha+\beta$ regions using (a) - SEM and (b,c) - TEM. In the SEM image, the arrows indicate the direction of the shear at the last pass of the ECAP.
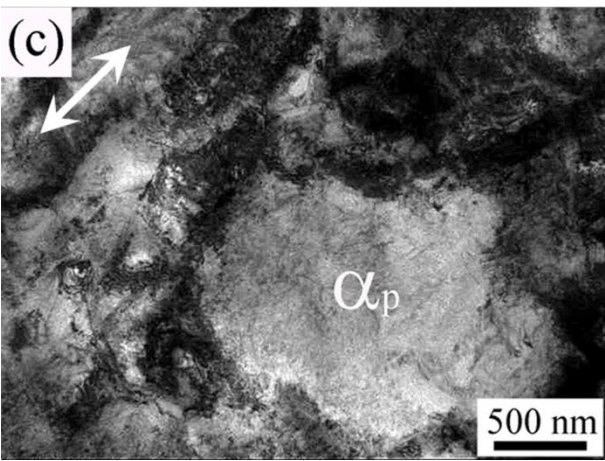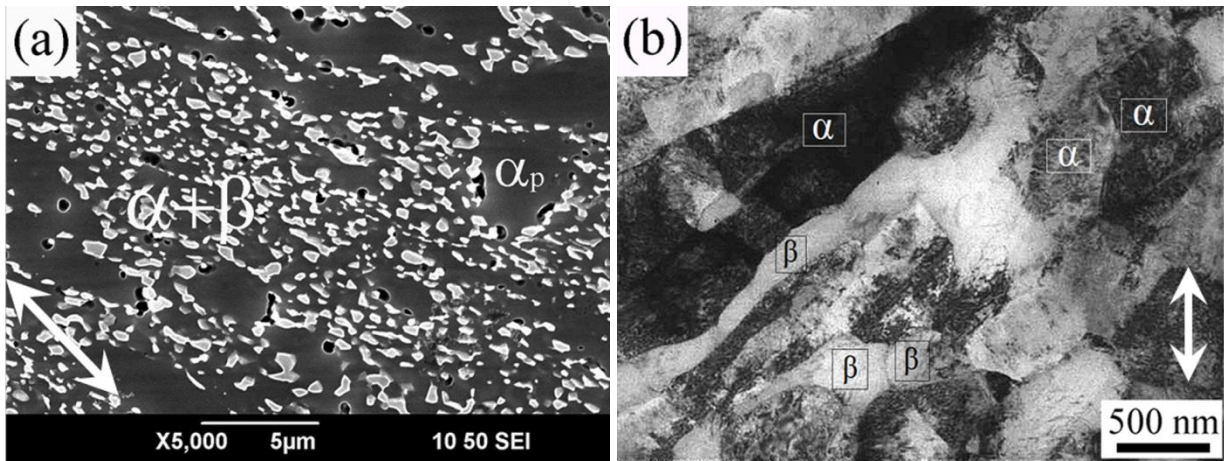
Fig. 7. Microstructure of the VT8M-1 alloy after ECAP processing for 4 passes: (a) - SEM and (b,c) - TEM.
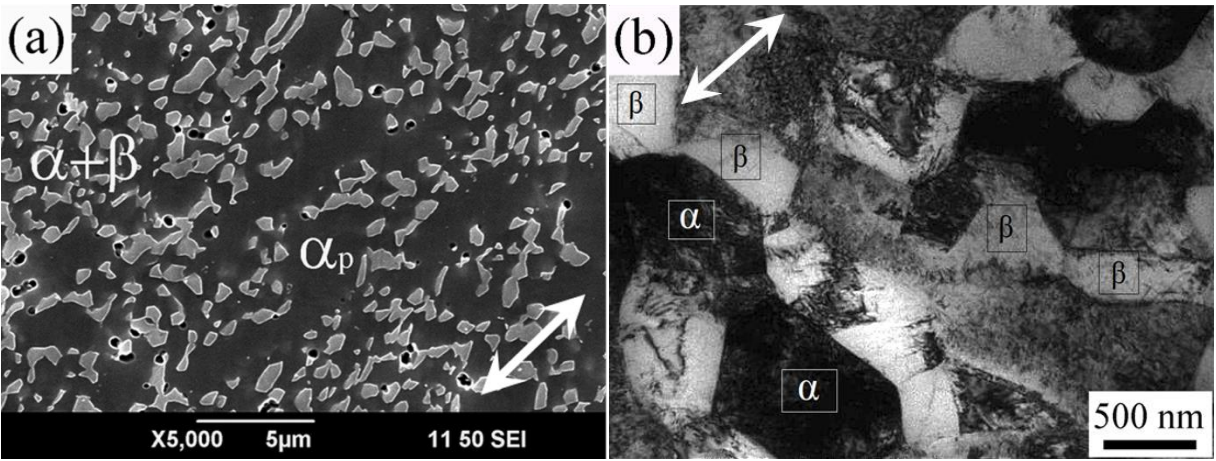
Fig. 8. Microstructure of the VT8M-1 alloy after ECAP processing for 6 passes: (a) - SEM and (b) - TEM.
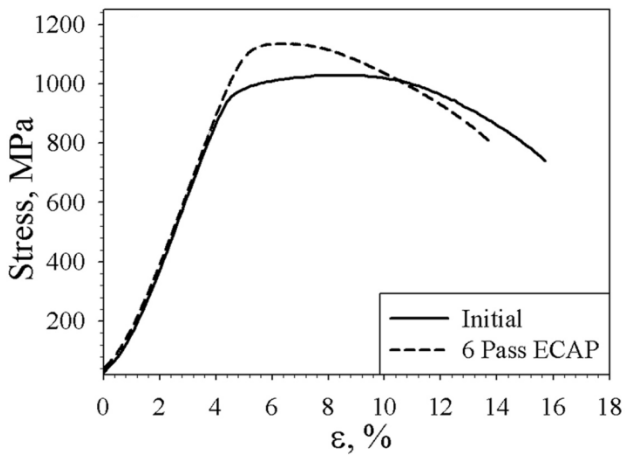
Fig. 9. Typical tensile curves of the VT8M-1 alloy with an initial duplex structure and after 6 ECAP passes.
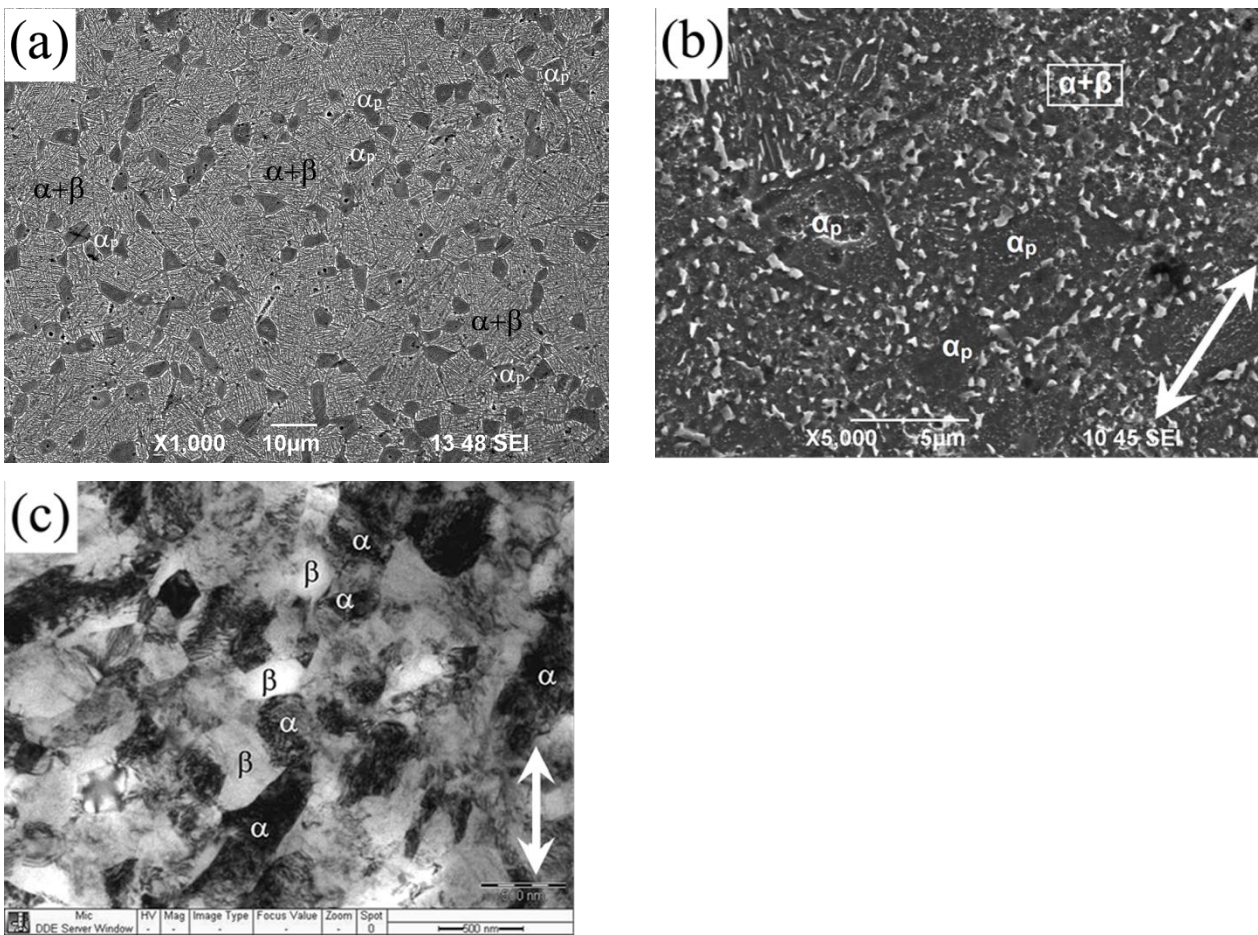
Fig. 10. Microstructure of Ti-6Al-4V alloy: (a) after preliminary heat treatment; b) after 6 ECAP passes at T=650°C; (c) TEM-images of the alloy UFG structure after 6 ECAP passes.

Fig. 11. The fraction of β-phase in Ti-6Al-4V and VT8M-1 alloys on the number of ECAP passes

Fig. 12. Dependence of ultimate tensile strength of Ti-6Al-4V and VT8M-1 alloys on the number of ECAP passes

Fig. 2. Microstructure of the VT8M-1 alloy after quenching at 940°C showing α_p and α'' regions: (a) - SEM and (b,c) - TEM.

19

Fig. 3. Globular-lamellar structure of the VT8M-1 alloy after heat treatment at 700°C for 1 hour using (a) - SEM and (b) - TEM.

Fig. 4. Engineering stress versus strain during compression of the VT8M-1 alloy at temperatures from 650 to 800°C using a strain rate of $1.4 \times 10^{-3} \, \text{s}^{-1}$ and corresponding microstructure.

Fig. 6. Microstructure of the VT8M-1 alloy after ECAP processing for 2 passes showing the α_p phase and $\alpha+\beta$ regions using (a) - SEM and (b,c) - TEM. In the SEM image, the arrows indicate the direction of the shear at the last pass of the ECAP.

21

Fig. 7. Microstructure of the VT8M-1 alloy after ECAP processing for 4 passes: (a) - SEM and (b,c) - TEM.

Fig. 8. Microstructure of the VT8M-1 alloy after ECAP processing for 6 passes: (a) - SEM and (b) - TEM.

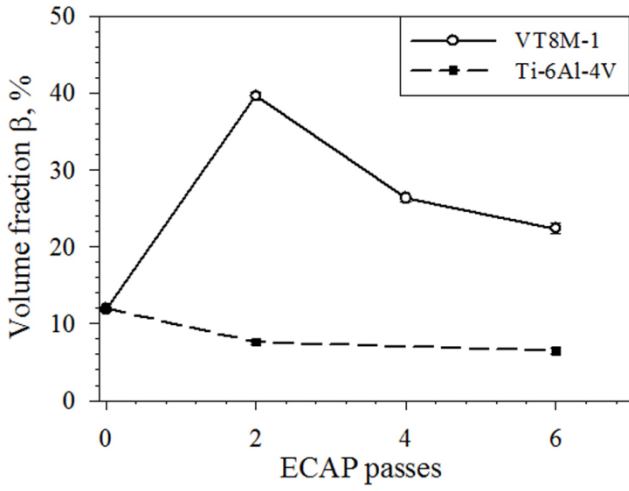Fig. 9. Typical tensile curves of the VT8M-1 alloy with an initial duplex structure and after 6 ECAP passes.

Fig. 11. The fraction of β-phase in Ti-6Al-4V and VT8M-1 alloys on the number of ECAP passes.
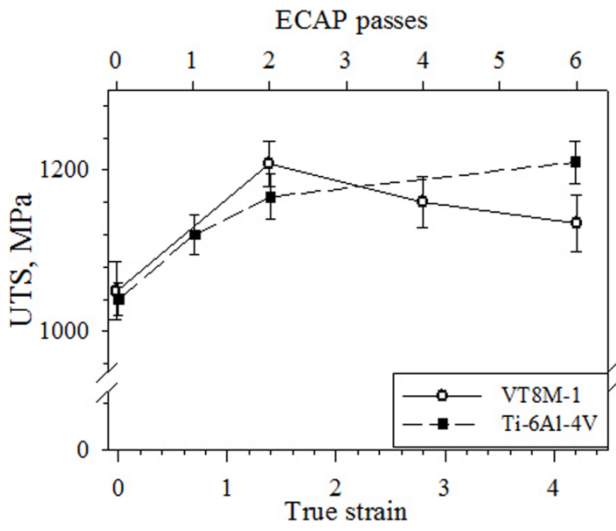

Fig. 12. Dependence of ultimate tensile strength of Ti-6Al-4V and VT8M-1 alloys on the number of ECAP passes.